Research Article

INTERNATIONAL JOURNAL OF CURRENT MEDICAL AND PHARMACEUTICAL RESEARCH

ISSN: 2395-6429, Impact Factor: 4.656
Available Online at www.journalcmpr.com
Volume 4; Issue 8(A); August 2018; Page No. 3575-3584
DOI: http://dx.doi.org/10.24327/23956429.ijcmpr20180514

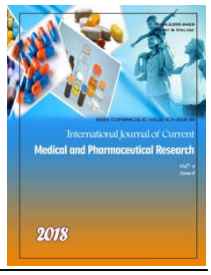

COMPARISON OF 3 TESLA MULTIPARAMETRIC PROSTATE MAGNETIC RESONANCE IMAGING FINDING AND HISTOPATHOLOGICAL FINDINGS IN THE DIAGNOSIS OF PROSTATE CANCER

HalimeÇomruk., Feyza GelebekYilmaz and Sakıp Erturhan

[1,2]Department of Radiology, Faculty of Medicine, Gaziantep University, Gaziantep, Turkey
[3D]epartment of Urology, Faculty of Medicine, Gaziantep University, Gaziantep, Turkey

ARTICLE INFO

Article History:
Received 22nd May, 2018
Received in revised form 5th June, 2018
Accepted 16th July, 2018
Published online 28th August, 2018

Key words:
Prostate Cancer, Multiparametric Magnetic Resonance Imaging (MpMRG), TRUS Biopsy, Clinically Significant Prostate Cancer

ABSTRACT

Aim: Our purpose was to evaluate the diagnostic performance of 3 T multiparametric MR imaging in prostate cancer detection by using histopathological findings as the reference standard, and to determine the potential utility of MpMR imaging for identification of clinically significant prostate cancer.

Matherial and methods: Between July 2017 and February 2018, 62 patients who underwent 3 Tesla (T) prostate MRI, were evaluated according to PIRADSv2 guidelines. All patients were scored by two radiologists blinded to pathology results, and then the correlation between PIRADSv2 scores and pathology results of 62 patients who had biopsy were analyzed.

Results: The mean age, PSA level and prostate volume of all patients were 65,6 years (46- 86), 70,81 (3.11-1170) ng/ml, 52,22 (7,9-161,7)ml, respectively. A statistically significant difference was found between PIRADS score of T2W, DWI, DCE, MpMRI and histopathological results ($p<0,05$). For T2W, the sensitivity was %83,87, the specifity was %61,29 (criteration>PIRADS 3, area under curve;0,73), for DWI the sensitivity was %93,55, the specifity was %80,65 (criteration> PIRADS 3, area under curve;0,87), for DCE the sensitivity was %93,55, the specifity was %67,74 (criteration for positive enhancement, area under curve;0,81). For MpMRI the sensitivity was %96,77, the specifity was %74,19 (criteration> PIRADS 3, area under curve;0,85). The ADC cut off value was found 0,7 x 10^{-3} mm^2/sec. ROC analysis was found for this cut off value area under curve;0,943, the sensitivity was %93,5, the specifity%83,9.

Conclusion: MpMRG appears to be very promising in identifying patients with suspected prostate cancer, localizing, characterizing, determining the level of risk, and determining patient selection and observation strategies for biopsy according to risk level.

INTRODUCTION

Prostate cancer is the most common cancer in males apart from skin cancers. It is the second leading cause of cancer-related deaths after lung cancer [1]. Studies show that one in 7 males has the risk of being diagnosed with prostate cancer in their lifetime [2].

Diagnosis of prostate cancer is based on the combination of prostate-specific antigen (PSA), digital rectal exam (DRE) and Transrectal Ultrasonography (TRUS)-guided multiple prostate biopsies [3]. PSA is a marker with high organ specificity but low cancer specificity. Serum PSA levels may also be elevated in benign cases such as nenign prostate hypertrophy (BPH), prostatitis and prostate manipulations (prostate massage, prostate biopsy) [4]. Cancer was detected in the biopsy of at least 1/3 of the males with suspected prostate cancer in DRE [5]. Generally, DRE is not solely used as a diagnostic method since it is a subjective evaluation and has low positive predictive value. Although TRUS especially contributes to reaching a histopathological diagnosis, it has a significant false negative rate [5]. The entire prostate might not be viewed using this method and the existing tumor can be missed although it is within the biopsy scheme. Advanced imaging modalities may play an important role in screening by classifying biopsies and enabling more targeted biopsies. Definitive diagnosis of prostate cancer can also be helpful in deciding whether to perform active follow-up or administer active treatment in selected cases[6].

Among radiological diagnostic methods, Magnetic Resonance Imaging (MRI) has been used since the 1980s as a non-invasive imaging modality in evaluating the prostate gland and the surrounding structures. In the beginning, prostate MRI was primarily used in staging of biopsy-proven cancers and identifying local spread and lymph node metastases since it only contained T1 weighted (T1W) and T2 weighted (T2W) classic sequences [7]. Due to the advances in technology (in

Corresponding author:* **HalimeÇomruk
Department of Radiology, Faculty of Medicine, Gaziantep University, Gaziantep, Turkey

terms of both software and hardware), Multiparametric Magnetic Resonance Imaging (MpMRI) has been developed with the combination of T2W in anatomical evaluation, Diffusion Weighted Imaging (DWI), Dynamic Contrast Enhanced Imaging (DCE-MRI) in functional evaluation, MR Proton Spectroscopy (MRS) and such other examinations (7). MpMRI plays an important role in diagnosing prostate cancer, identifying the localization and in staging[8].

After prostate MRI became widespread, some differences emerged in imaging parameters, in interpreting and reporting the images. In 2015, ACR and ESUR published Prostate Imaging and Reporting and Data System v2 (PI-RADS v2) guidelines in order to create the minimum acceptable technical parameters for MpMRI, provide standardization interminology, interpretation and reporting, to increase the rates of lesion detection, localization, characterization and risk level assessment in patients with suspected prostate cancer [9]. The objective of our study is to investigate the correlation between histopathology results and MpMRI findings that were obtained, interpreted and reported according to the recommendations of PI-RADS v2 system before performing TRUS-guided biopsy in patients with suspected prostate cancer.

MATERIALS AND METHODS

The study included 62 patients that were scheduled to undergo TRUS-guided biopsy due to the presence of positive examination or laboratory findings indicating prostate cancer found in the Department of Urology between July 2017-February 2018 and that underwent MpMRI for prostate cancer screening and diagnosis purposes in 3 Tesla (T) Ingenia (Philips, Hollanda) MR device in the Radiology Department before the biopsy. Patients with marked hemorrhage intensities in the prostate parenchyma were not included in the study. In our study, ethical consent was obtained; however, informed consent was not obtained from the patients since the study is retrospective.

As a result of evaluating the clinical, laboratory and imaging findings, 57 TRUS-guided 10 quadrant biopsies, 1 TRUS-guided 22 quadrant saturation biopsy were performed and images of 62 patients in total also including 4 patients with prostatectomy material were analyzed in PACS (Picture Archiving Communication Systems) and PI-RADS v2 scores were compared with histopathological findings.

Multiparametric Magnetic Resonance Imaging Technique

All prostate scans within the scope of the study were performed in Philips Ingenia (Medical Systems, Best, Netherlands) MRI unit with 3T magnetic field without using endorectal coil (ERC) with a 32-channel pelvic coil (pelvic multichannel phased-array coil). Care was taken not to have patients' rectum and bladder full since it makes it harder to evaluate prostate and seminal vesicles.

Axial T1W, axial-coronal-sagittal T2W, axial DWI, and axial fat-suppressed DCE-MRI sequences were obtained in a manner to encompass the seminal vesicle and the entire prostate, and pelvic axial T2W SPAIR and pelvic postcontrast fat-suppressed T1W sequences from the aortic bifurcation to symphysis pubis were obtained for evaluating the pelvic lymph node and metastases.

Diffusion weighted images were obtained from 3 axial plane echo-planar images (EPI) in total by taking 3 different b values (b: 0-1000-1500 s/mm2). ADC maps were automatically created by the device (Table1).

DCE-MRI; after 1 image was obtained without using contrast agent, a total of 8 images were obtained following bolus administration of 0.2 ml/kg contrast containing gadolinium with auto-injector via the antecubital vein at 3 ml/s. Post-processing subtraction images were automatically created.

Table 1 Prostate MRI scanning protocol (3T Philips Ingenia)

	Sequence	Section thickness (mm)	Field of view (mm)	TE (ms)	TR (ms)	gap (mm)	b value	Flip angle
T2W axial	TSE	3	180x180	120	5538	0,3		90
T2W coronal	TSE	3	180x180	120	4341	0,3		90
T2W sagittal	TSE	3	180x180	120	5788	0,3		90
SPAİR	TSE	5	300x300	80	4967	1		90
T1W axial	TSE	3	160x160	9	572	0		90
DWI	SE-EPI	3	250x214	87	5177	3	0,1000,1500	90
DCE	DYN THRIVE	3	375x299	1,48	3,1	0		10
T1W postcontrast	THRİV E	3	375x299	1,48	3,1	0		10

THRIVE: Tl High-Resolution Isotropic Volume Excitation, TE: time of echo, TR: time of repetition, SPAİR: SPectral Attenuated Inversion Recovery, SE-EPI = spin-echo echo-planar imaging,

Respiratory trigger was used in order to reduce the respiratory artifacts in T2A images, DWI and DCE-MRI.

Radiologic Evaluation

Prostate MR images were evaluated by one senior-year radiology assistant and one radiologist with experience in abdominal imaging by taking the PI-RADS v2 guidelines as a basis and by knowing the PSA value but not the biopsy results of the patients.

The base was determined to be the region extending from the cranial margin of the prostate to the widest transverse diameter of the prostate. The midgland was defined as theregion between the widest transverse diameter and the vermorantum, which is the level where ejaculatory ducts unite and open to the mid-section of prostatic urethra. The apex was defined as the region inferior to the midgland. Prostate volume was manually calculated as [(maximum anterior-posterior diameter) x (maximum transverse diameter) x (maximum longitudinal diameter) x 0.52].

T1W images were reviewed first in order to distinguish a possible hemorrhage in the prostate and seminal vesicles. Lesions were scored from 1 to 5 based on PI-RADS v2 guidelines by their images in T2W and DWI by indicating the appearance and size of the lesions in the transition zone and peripheral zone. Dynamic contrast enhanced images were evaluated as "negative" or "positive". Then, MpMRI PI-RADS assessment category of the lesions was scored from 1 to 5 with the combination of all images. Finally, PI-RADS assessment category of the index (dominant) lesion was specified. If the number of lesions with the highest PI- RADS assessment category is more than one, the lesion that extends beyond the prostate was considered the index lesion. If the smaller of two lesions with the same PI-RADS assessment category extends beyond the prostate, the small lesion was considered as the index lesion regardless of the size and dimensions of the other lesion. If none of the lesions within the prostate extend beyond the prostate, the largest lesion with the highest PI-RADS assessment category was considered the index lesion.

The mean ADC value of the index lesion was measured by manual placement of more than one ROI (region of interest) in 3 different areas which had the most distinct hypointensity in the ADC map and the most distinct hyperintensity in the diffusion sequence that corresponds to the lesion in DWI at the work station. The lowest value among these mean ADC values was taken as the mean ADC value of the lesion.

Index lesions were grouped as high risk (PI-RADS 4 or 5) or low risk (PI-RADS 1, 2 and 3) according to PI-RADS v2. Lesions were evaluated from T2W and fat suppressed contrast enhanced T1W images with high spatial resolution in terms of extraprostatic extension, invasion of the neurovascular bundle, invasion of seminal vesicle or other organs.

In terms of lymph node metastasis, paraaortic lymph node stations at obturator, external iliac, internal iliac, common iliac, pararectal, presacral and bifurcation level were evaluated from T2W SPAIR and fat suppressed postcontrast T1W images. Spherical lymph nodes with a short axis longer than 8 mm without the presence of fatty hilum were interpreted as pathological lymph nodes. In addition, these images were analyzed so as to determine if there were any musculoskeletal metastases.

Histopathological Evaluation

Within the scope of the study, 57 transrectal ultrasonography-guided 10 quadrant biopsies, and 1 TRUS-guided 22 quadrant saturation biopsy were performed and prostate pathology results of 62 patients in total, also including 4 patients with prostatectomy material, were analyzed. Pathologically, lesions with a tumor volume of 0.5 cc and above, Gleason score of 3+4 and above (ISUP grade 2 and above), and with extraprostatic extension were accepted as CSC.

Statistical Analysis

The Shapiro Wilk test was used to check the normal distribution of the numerical variables. Student t test was used in comparing 2 independent groups for variables with normal distribution, and Mann Whitney U test was used for variables without a normal distribution. ROC analysis was applied to determine the cutoff value for diagnostic tests. Sensitivity, specificity and 95% confidence intervals were calculated as diagnostic test efficacy statistics.

Chi-square test was used in the comparison of categorical variables. SPSS for Windows version 22.0 and Medcalc 17.5.5 software packages were used for statistical analyses, and P< 0.05 was considered statistically significant.

RESULTS

Sixty-two patients who underwent Multiparametric Magnetic Resonance Imaging were included in the study. Patients' ages were between 46 and 86 (65.13 ± 6.8) and PSA values were between 3.11 and 1170 ng/ml (70.8±198.2 ng/ml). The mean prostate gland volume was 52.2±32.2 cm^3. Age and PSA values of the patients who had positive pathology results for clinically significant cancer were significantly higher than those with negative results (p=0.001). Prostate volumes of the patients who had positive pathology results for clinically significant cancer were significantly lower than those with negative results (p=0.002). Analyzing the T1W images, 17 patients (27.4%) had hemorrhage, whereas 45 patients (72.6%) did not have hemorrhage. Among 62 patients who underwent biopsy or prostatectomy, 31 (50%) had Clinically Significant Cancer (CSC) and 4 of those originated from the transition zone (12.9%) and 27 from the peripheral zone (87%). Reviewing the pathology results of 62 patients who underwent biopsy or prostatectomy, 31 (50%) were reported as prostatic adenocarcinoma, 1 (1.6%) was reported as micro adenocarcinoma, 4 (6.4%) were reported as chronic prostatitis, 2 (3.22%) as ASAP, and 24 (38.7%) as normal prostate tissues. After the biopsy performed on the patient who had micro adenocarcinoma, Gleason score was reported as 3+3.Among 32 patients with malignant pathology results, 1 was reported as Gleason 6(3.1%), 15as Gleason 7(46.8%), 7asGleason 8(21.8%) and 9 as Gleason 9 (28.1%).

Among the patients that had PI-RADS 5 lesions in MpMRI, extraprostatic extension was detected in 17 patients, invasion of the seminal vesicle in 15 patients, invasion of the neurovascular bundle in 5 patients, bladder invasion in 1 patient and bone metastasis in 3 patients. In 14 of the 38 patients that had lesions assessed as high-risk (PI-RADS 4 and 5) in MpMRI according to PI-RADS v2, several (multifocal) lesions with malignant appearance were observed in the prostate. Among these patients with multifocality, 13 had CSC and 1 did not have CSC.

Evaluating the presence of periprostatic lymph nodes in MpMRI, pathological pelvic lymph node was detected in the areas neighboring the prostate in 11 (17.7%) patients and not detected in 51 (82.3%) patients. Among the patients that had pathological lymphnode according to the MpMRI, CSC was histopathologically detected in 10 patients, and 1 was reported as normal prostate tissues.

Reviewing the T2 Weighted images, 11 patients (17.7%) were scored P2, 13 patients (20.9%) P3, 11 patients (17.7%) P4, and 27 patients (43.5%) P5. There was no P1 score. When T2W score cutoff value was taken as > PI-RADS 3, area under the curve in ROC analysis curve was found to be 0.73. 95% confidence interval for this area is 0.60-0.83. Area under the curve is statistically significant (p<0.05). For T2W, sensitivity was found 83.57%, specificity 61.29%, positive predictive value 62.42%, and negative predictive value 79.17%. (Table2).

Table 2 Analysis of high or low T2W scores according to PI-RADS v2 in terms of clinically significant cancer

			Pathology		
			CSC(-)	CSC(+)	Total
T2Wscore GROUP	low risk (≤P3)	number	19	5	24
		%	61,3%	16,1%	38,7%
	high risk (P4andP5)	number	12	26	38
		%	38,7%	83,9%	61,3%
TOTAL		number	31	31	62
		%	100,0%	100,0%	100,0%

Reviewing the Diffusion Weighted images, 19 patients (30.6%) were scored P2, 8 patients (12.9%) P3, 8 patients (12.9%) P4, and 27 patients (43.5%) P5. When DWI score cutoff value was taken as > PI-RADS 3, area under the curve in ROC analysis curve was found to be 0.87. 95% confidence interval for this area is 0.76-0.94. Area under the curve is statistically significant (p<0.05). For DWI, sensitivity was found as 93.55%, specificity as 80.65%, positive predictive value as 82.86%, and negative predictive value as 92.59%. (Table 3)

Table 3 Analysis of high- or low-risk DWI scores according to PI-RADS v2 in terms of clinically significant cancer

			CSC(-)	CSC(+)	Total
DWISCORE GROUP	low risk (≤P3)	Number	25	2	27
		%	80,6%	6,5%	43,5%
	high risk(P4 and P5)	Number	6	29	35
		%	19,4%	93,5%	56,5%
TOTAL		Number	31	31	62
		%	100,0%	100,0%	100,0%

Reviewing the dynamic contrast enhanced MR images, 39 patients (62.9%) were assessed to be positive and 41 patients (37.1%) negative according to PI-RADS v2 guidelines. For dynamic contrast enhanced MR imaging (DCE-MRI), area under the curve in ROC analysis curve was found to be 0.81. 95% confidence interval for this area is 0.69-0.90. Area under the curve is statistically significant (p<0.05). For DCE-MRI, sensitivity was found as 93.55%, specificity as 67.74%, positive predictive value as 74.36%, and negative predictive value as 91.96% (Table 4).

Table 4 Analysis of positive and negative contrast agent uptake according to PI-RADS v2 in terms of clinically significant cancer

			Pathology		
			CSC(-)	CSC(+)	Total
DCE-MRI	Negative	Number	21	2	23
		%	67,7%	6,5%	37,1%
	Pozitive	Number	10	29	39
		%	32,3%	93,5%	62,9%
TOTAL		Number	31	31	62
		%	100,0%	100,0%	100,0%

In the MpMRI assessment constituted by the combination of T2W, DWI and DCE-MRI findings, 15 patients (24.1%) were scored P2, 9 patients (14.5%) P3, 11 patients (17.7%) P4 and 27 patients (43.5%) P5 according to PI-RADSv2 guidelines. When PI-RADS score cutoff value of MpMRI, which is constituted by the combination of T2W, DWI and DCE- MRI findings, was taken > PI-RADS 3, and the area under the curve in ROC analysis curve was found to be 0.85. 95% confidence interval for this area is 0.74-0.93. Area under the curve is statistically significant (p<0.05). For MpMRI, sensitivity was found as 96.77%, specificity as 74.19%, positive predictive value as 78.95%, and negative predictive value as 95.83% (Table5).

Table 5 Analysis of high- or low-risk PI-RADS scores according to PI-RADS v2 in terms of clinically significant lesions

			Pathology		
			benign	Malign	Total
MpMRG GROUP	Low risk (≤P3)	Number	23	1	24
		%	74,2%	3,2%	38,7%
	High risk (P4 and P5)	Number	8	30	38
		%	25,8%	96,8%	61,3%
Total		Number	31	31	62
		%	100,0%	100,0%	100,0%

Sensitivity, specificity, PPV and NPV values for MpMRI, T2W, DWI and DCE-MRI were compared in table 6.

Table 6 ROC analysis for MpMRI, T2A, DWI, DCE-MRI

Variables	AUC	%95 Confidence Interval	Sensitivity (%)	Specificity (%)	Positive Predictive Value (%)	Negative Predictive Value (%)
MpMRG	0,85	0,74 - 0,93	96,77	74,19	78,95	95,83
T2W	0,73	0,60 - 0,83	83,87	61,29	68,42	79,17
DAG	0,87	0,76 - 0,94	93,55	80,65	82,86	92,59
DCE-MRI	0,81	0,69 - 0,90	93,55	67,74	74,36	91,30

ADC values of the patients who had positive pathology results for clinically significant cancer were significantly lower than those with negative results (p=0.001), wherein in investigating a cutoff value for mean ADC value in patients diagnosed with prostate cancer, area under the curve was found to be 0.943. 95% confidence interval for this area is 0.85-0.98. Area under the curve is statistically significant (p<0.001). The cutoff value for ADC was found to be 0.7 x 10^{-3} mm^2/s, and accordingly, the sensitivity and specificity of the mean ADC value was 93.5% and 83.9%, respectively (Figure1).

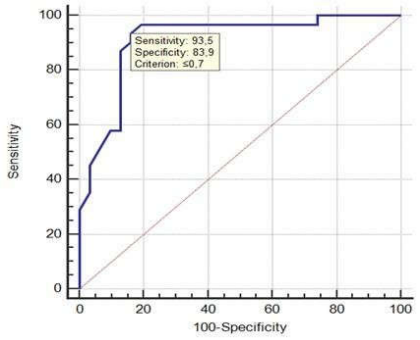

Figure 1 ROC curve for the cutoff value determined in order to detect clinically significant cancer

DISCUSSION

Prostate cancer is the most common cancer in men in the USA [10]. Studies show that one in 7 males has the risk of being diagnosed with prostate cancer in their lifetime [2].

Prostate cancer can exhibit extremely heterogenous behavior. It may stay silent for a long time or be very aggressive. Therefore, determination of tumor behavior is as important as the diagnosis. This is because the extreme increase in the number of diagnoses results in diagnosing and overtreating tumors that are clinically insignificant and that can stay silent for long years. Preventing this can be possible by differentiating between clinically insignificant cancers and cancers that can progress aggressively. Today, with the use of digital rectal exams in conjunction with PSA and its derivatives in diagnosis, it was found that prostate cancer specific mortality was reduced, however the number of biopsies increased 70-80% [11]. Because, PSA is a marker with high organ specificity but low cancer specificity. Serum PSA levels might be elevated in benign cases other than cancer[11]. Due to lowering PSA threshold values and applying intense PSA scanning programs to detect the disease when it is curable and limited to the organ, the importance of systematic prostate biopsy has significantly improved as the lesions that are expected to be found were very small to detect using only TRUS and nearly 40% were iso-echoic in TRUS. Moreover, because of the vicious cycle in the effort to detect the disease early, the specificity is lost and the number of negative biopsies is significantly increased. Despite all these efforts, 20-30% of cancer cases still cannot be recognized and biopsies are repeated since the reason for biopsy is elevated PSA level [12. 13].New cancer cases are detected with each

new biopsy; however, the rate of cancer detection in repeated biopsies gradually decreases [14]. Each repeated biopsy performed with increased number of samples renders the procedure more painful and less tolerable. Djavan *et al*.[15] reported that the pain in the first two biopsies was expressed as tolerable, whereas especially younger patients (below 60) expressed higher discomfort in the third and fourth biopsyprocedures.

The contemporary diagnostic approach consisting of the PSA test, digital rectal exam followed by TRUS-guided biopsy has low sensitivity and specificity in the diagnosis of PCa. Furthermore, this diagnostic approach provides limited information about the aggressiveness and stage of cancer and leads to misclassification of the risk. Risk misclassification results in including the patients in a lower risk group and administering inadequate treatment and may consequently lead to increased relapse/recurrence rate or overtreatment of patients who may be recommended to stay under active follow-up due to the concern of understaging [16].

The main purpose of prostate MRI examination is to define and localize anomalies that correspond to clinically significant prostate cancer. “Clinically significant cancer (CSC)” has been defined in order to standardize MpMRI reports with PI-RADS v2 and to ensure the pathological correlation in clinical-study practices. Cancers that have a Gleason score of 7 and above (including marked but not dominant 3+4 with Gleason 4 component) according to pathology results, and/or volume 0.5 cc and above and/or extraprostatic extension is defined as CSC [7]. In PI-RADS v2 assessment, probability is predicted over 5 points in terms of CSC for each lesion in the prostate gland according to the combination of T2W, DWI and DCE- MRI findings [7].This system enables creating the risk assessment categories of the cases and determining observation and patient selection strategies for biopsy[7].

High-resolution T2W examination is a significantly important sequence in evaluating anatomy, detecting tumors larger than 0.5 cc, determining tumor localization and local staging. In a study conducted by Panebianco *et al*. [17] on 1140 patients, the sensitivity, specificity, positive predictive value, negative predictive value and the area under the curve for T2A imaging only were found as 67%, 73%, 89%, 61% and 0.80, respectively. In our study, sensitivity was found as 83.57%, specificity as 61.29%, positive predictive value as 62.42%, negative predictive value as 79.17% and the area under the curve as 0.73. The specificity of solely T2W images is significantly low. This is because hemorrhage, chronic prostatitis, scar, atrophy, radio and hormonotherapy also result in hypointensity in the peripheral zone in T2W images and this decreases the specificity of this method. T2W images, which have relatively high sensitivity and low specificity, should be combined with functional sequences in order to increase their performance in the diagnosis of PCa [18].

Diffusion Weighted Images and ADC values play an important role in lesion characterization and in assessing the aggressiveness of the tumor. Prostate cancer damages glandular tissue and replaces the tubules. Cell density of tumor tissue is higher than a healthy peripheral zone and low ADC values in comparison with the surrounding normal tissue are frequently observed in the ADC map. In a meta-analysis published by Lian-Ming Wu *et al*. [19], it was stated that the sensitivity (54-98%) and specificity (58-100%) of the T2W images in the diagnosis of prostate cancer were increased with the combination of T2W and DWI. In a study by Yoshimitsu *et al* [20], it was reported that there was a significant difference between the ADC values of well and poorly differentiated prostate cancers and there was a slight but significant connection between the ADC value and the histologic grade of prostate cancer. DeSouza *et al* [21] have shown that there is a significant difference between tumor ADC values of patients with low-risk local disease (Stage ≤T2a and Gleason score<7 and PSA<10 ng/mL) and patients with moderate or high risk disease (Stage ≥T2b and/or Gleason score ≥7 and/or PSA>10ng/mL).

In various publications, different cutoff values of ADC were determined due to the use of devices with different features and use of different b values [22- 24]. In our study, the cutoff value for ADC was found as 0.7 x 10^-3 mm2/s in ROC analysis and according to this value, the area under the curve in ROC analysis of the ADC value is statistically significant ($p<0.001$).

As a result of their study, Yoshimitsu *et al*. [20] asserted that ADC values in prostate cancer were inversely proportional to the increased cell density of the tumor and histologic Gleason score and therefore these values could be used in assessing tumor aggressiveness in a noninvasive manner. According to our study, there was no correlation between Gleason score and ADC values ($p=0.119$). However, ADC values of the patients who had positive pathology results for clinically significant cancer were significantly lower than those with negative results ($p=0.001$).

In several publications, the sensitivity and specificity of DWI in the diagnosis of PCa were reported as 54-94% and 61-100%, respectively [20, 25, 26]. Although sensitivity and specificity of DWI are higher as compared to T2W and DCE-MRI, T2W and DCE-MRI are more important sequences in local staging. DWI has to be combined with other sequences for local staging.

In our study, sensitivity was found as 93.55%, specificity as 80.53%, positive predictive value as 82.86%, negative predictive value as 75.71% and the area under the curve as 0.87 for DWI, which are all consistent with the literature.

According to PI-RADS v2, “positive” contrast uptake in DCE-MRI is defined as a lesion that has focal contrast uptake simultaneous with or earlier than the surrounding normal prostate tissue and that has a corresponding lesion in T2W and DWI. The sensitivity and specificity of DCE-MRI in tumor detection are within the range 46-96% and 74-97%, respectively. These values vary according to patient selection, technique, analysis limitations of images, pathological evaluation material (biopsy / radical prostatectomy) or tumor volume [27, 28]. In our study, sensitivity and specificity for DCE-MRI were found as 93.55% and 67.74%, respectively, which are consistent with the literature.

Since benign lesions such as BPH nodules with high vascularization in the transition zone, ectopic stromal nodule, and chronic prostatitis in the peripheral zone have a contrast uptake similar to PCa, the specificity of DCE-MRI in the diagnosis of prostate cancer is low (Figure 2, 3, 4).

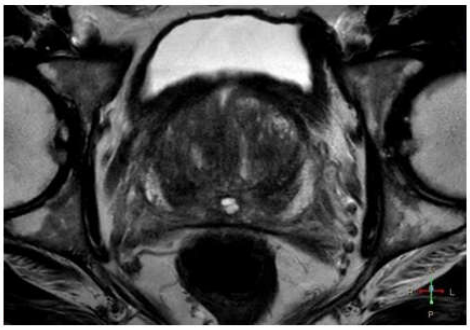

a

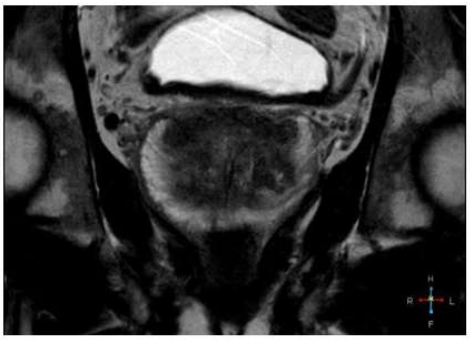

b

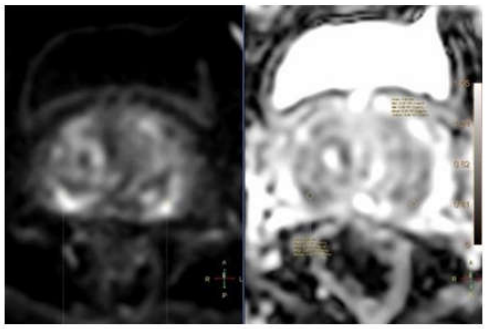

c

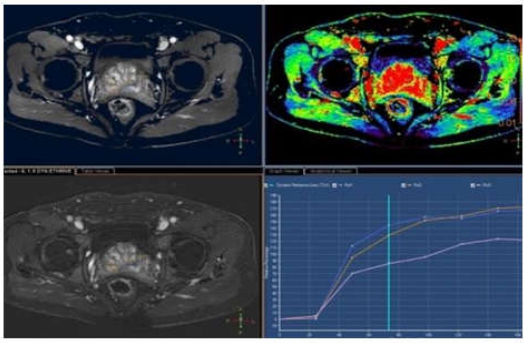

d

Figure 2 MpMRI examination of a 64-year-old patient with PSA 29 ng/ml; when bilateral symmetrical hypointense areas described in the ejaculatory duct periphery were evaluated in conjunction with coronal T2W images, they were assessed as compressed central zone due to enlarged transition zone (dumbbell sign). Chronic prostatitis was reported after TRUS-guided biopsy. **a)** Axial T2W examination; hypointense areas (arrow) with regular margins and symmetrical localization are observed in the bilateral posterior peripheral zone at prostate base level (T2W score P4). **b)** Coronal T2W examination; Hypointense area (arrow) with relatively regular margins is observed in the superior transition zone at prostate baselevel.
c) DWI with b1500; Hypointense areas in T2W images were luminous in the diffusion sequence and hypointensity was observed in the ADC map. In the ADC map, mean ADC value of the right hypointense area and left hypointense area were measured as 0.69 and 0.89, respectively (DWI score P4). **d)** According to DCE-MRI, early and rapid contrast uptake was observed in the areas consistent with T2W and DWI (Contrast uptake "+").

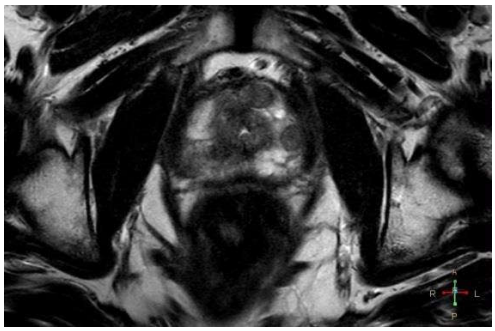

a

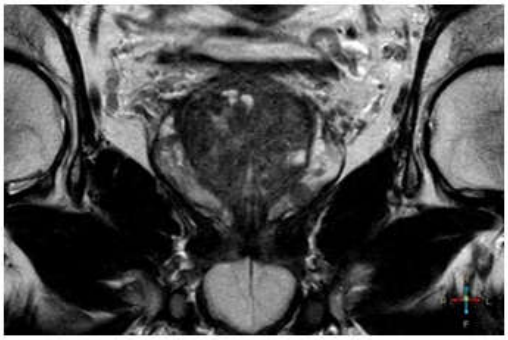

b

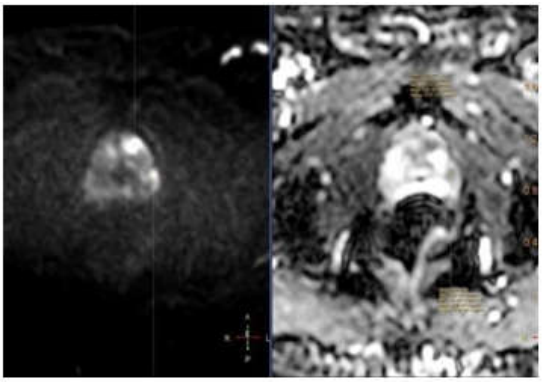

c

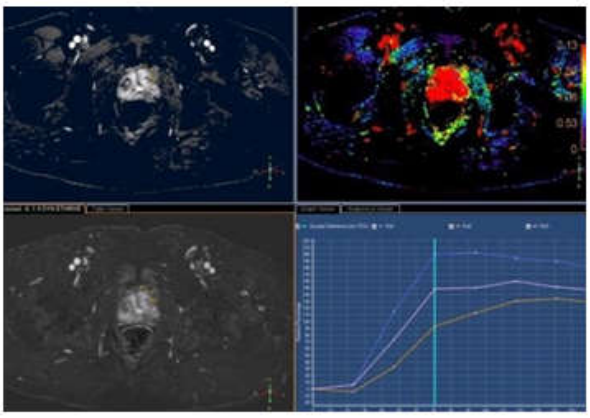

d

Figure 3 MpMRI examination of a 71 year-old patient with PSA 6.48 ng/ml; the lesion described below was assessed as a peripheral zone lesion. Lesion was assessed as an ectopic BPH nodule due to its nodular appearance with regular margins and the presence of a thin rim-shaped hypointense area consistent with the capsule around the lesion. PI-RADS score was determined as 2. Normal prostate tissues were reported after TRUS-guided biopsy. **a)** Axial and **b)** coronal T2W examination; 2 nodular hypointenseheterogenous areas with regular margins are observed in the left anterior and lateral peripheral zone at prostate apex level (T2W score P3). **c)** DWI examination; the described lesions are luminous in DWI and hypointensity is observed in the ADC map. Mean ADC value of the lesion in the anterior and posterior were measured as 0.75 and 0.95, respectively (DWI score P4). **d)** DCE-MRI examination; Lesions exhibited increased contrast uptake as compared to the neighboring peripheral zone (Contrast uptake "+").

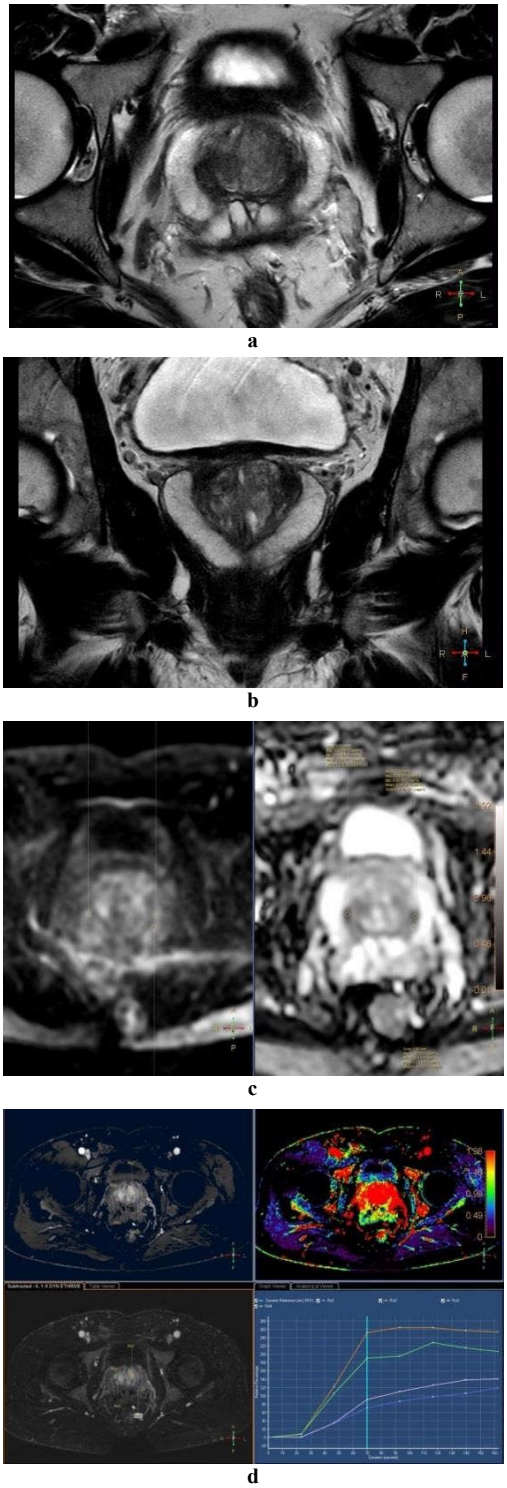

Figure 4 MpMRI examination of a 47-year-old patient with PSA 4.87 ng/ml; the areas described below were assessed as the thickening of the surgical capsule due to typical localization and appearance and the score was determined to be PI-RADS 2. Normal prostate tissues were reported after TRUS-guided biopsy. **a)** In axial and **b)** coronal T2W examination, crescent-shaped hypointense areas (arrows) with regular margins surrounding the right and left transition zone were observed at prostate base level (T2W score P4). **c)** DWI with b1500; hypointense areas do not exhibit marked restriction in DWI, hypointensity is observed in the ADC map. In the ADC map, the mean ADC value of the right hypointense area and the left hypointense area were measured as 0.58 and 0.68, respectively (DWI score P2). **d)** In DCE- MRI examination, lesions have less contrast uptake as compared to the transition zone (Contrast uptake"-").

DCE-MRI and T2W imaging are significantly important sequences in detecting extraprostatic extension, seminal vesicle, neurovascular bundle, bladder wall, rectum invasion and bone metastasis, and we experienced this in our study especially with DCE-MRI sequences (Figure 5, 6).

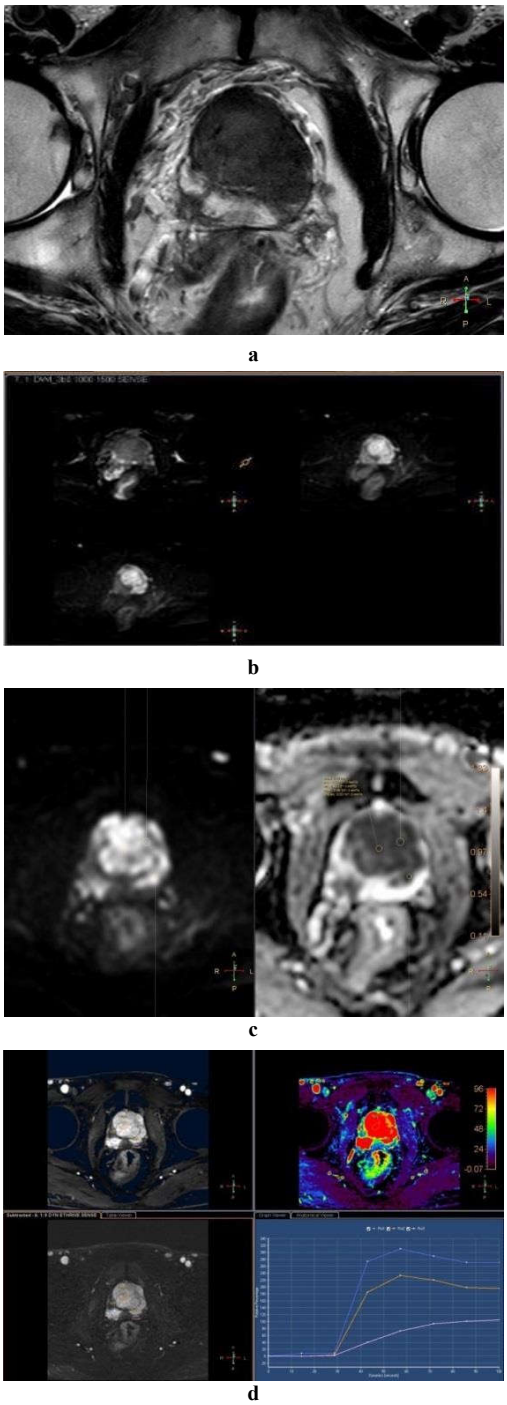

Figure 5 MpMRI examination of a 71-year-old patient with PSA 115 ng/ml; the index lesion described below was assessed as a transition zone lesion and its score was determined to be PI-RADS 5. After the TRUS-guided biopsy, Gleason score was reported as 4+3 for prostatic adenocarcinoma. **a)** Axial T2W examination; Hypointense lesion (arrow) with irregular margins that results in extraprostatic extension in the left lateral capsule was observed in the transition zone and left peripheral zone at prostate midgland level. In addition, hypointense lesion with a smaller size that extends to the neighboring right NVD (arrow head) in the left posterolateral peripheral zone was observed at this level (T2W score P5). **b)** In the DWI with a value of b1500, lesions were luminous **c)** the mean ADC value was measured as 0.46 in the ADC map (DWI score P5). **d)** According to DCE-MRI, intense contrast uptake and wash out were observed in suspected areas in T2W and DWI (Contrast uptake"+").

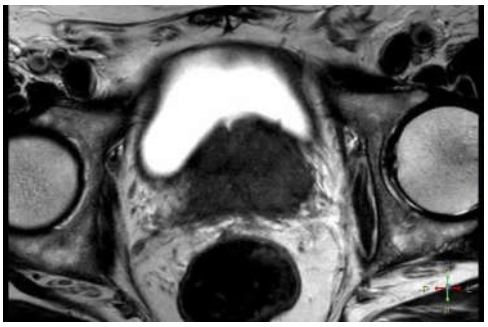

a

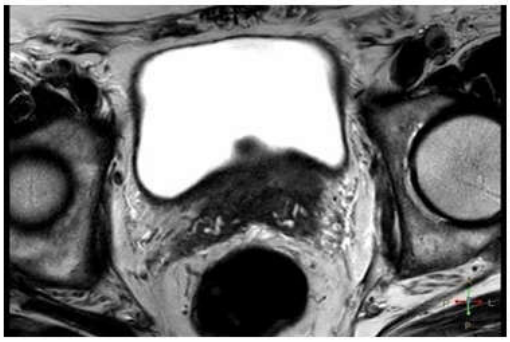

b

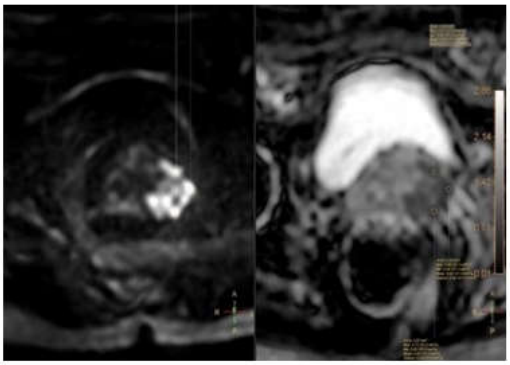

c

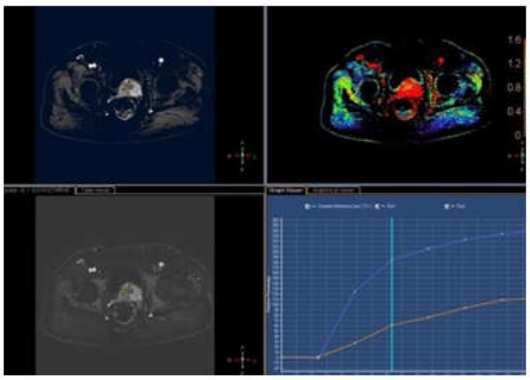

d

Figure 6 MpMRI examination of a 68-year-old patient with PSA 3.11 ng/ml; the lesion described below was assessed as a peripheral zone lesion that exhibits bilateral invasion of the seminal vesicle and extraprostatic extension and the score was determined to be PI-RADS 5. After the TRUS-guided biopsy, Gleason score was reported as 4+5 for prostatic adenocarcinoma. **a)** Axial T2W examination; diffuse hypointense lesion (arrow head) with irregular contours that extends to extraprostatic adipose tissue was observed in the transition zone and peripheral zone at prostate base level (T2W score P5). **b)** Lesion showed bilateral invasion of the seminal vesicle, which is more marked on the left side (arrow). **c)** In the DWI with a value of b1500, restriction in the left posterolateral peripheral zone at prostate base level was observed in DWI, the mean ADC value of this area in the ADC map was measured as 0.55 (DWI score P5). **d)** DCE-MRI examination; early contrast uptake was observed in the left posterolateral peripheral zone at prostate base level in comparison to the neighboring peripheral zone (Contrast uptake "+").

Although parameters used in the MRI provide important findings alone, evaluation of T2W images in conjunction with two functional images provides better results in detecting clinically significant cancer and revealing its characteristics [29 ,30]. In a meta-analysis published by Fütterer *et al*. [31] in 2015, the sensitivity, specificity, positive predictive value, and negative predictive value of MpMRI in detecting clinically significant cancer were reported within the range 58-96%, 23-87%, 34-68% and 63-98%, respectively. In a study by Abd-Alazeez *et al*. [32], when PI-RADS 4 score was taken as the threshold value for positive MpMRI, the sensitivity, specificity, and negative predictive value were reported as 92%, 61% and 99% respectively. In our study, sensitivity was found as 96.77%, specificity as 74.19%, positive predictive value as 78.95%, negative predictive value as 95.83% for MpMRI, which are all consistent with theliterature.

One of the most important contributions of multiparametric MRI is that it reveals extraprostatic extension and local recurrence. This is because extension beyond the capsule and involvement of the seminal vesicle, which are among the extraprostatic extension criteria, are independent pathologic criteria that increase local recurrence, progression and death risk. In these cases considered high-risk, the possibility of local recurrence is 40-50% [33]. In a study by Park *et al*. [34], the sensitivity and specificity of MRI in terms of extraprostatic extension were found 75% and 92%, respectively. In our study, among the patients that had PI-RADS 5 lesions in MpMRI, extraprostatic extension was detected in 17 patients, invasion of the seminal vesicle in 15 patients, invasion of the neurovascular bundle in 5 patients, bladder invasion in 1 patient and bone metastasis in 3 patients (Figure 7).

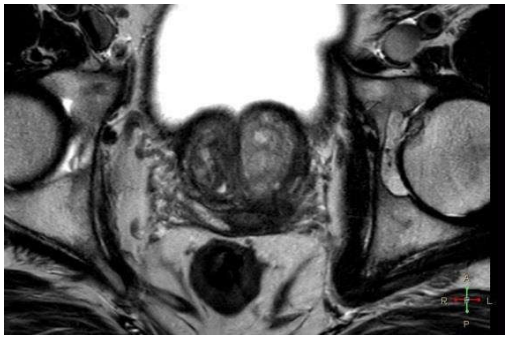

a

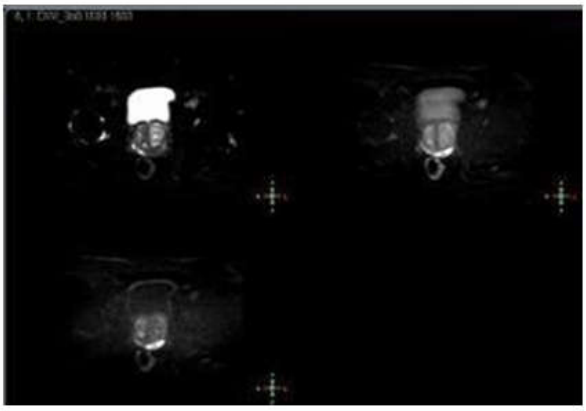

b

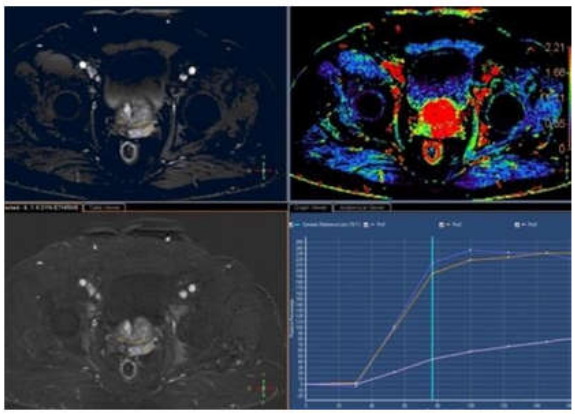

c

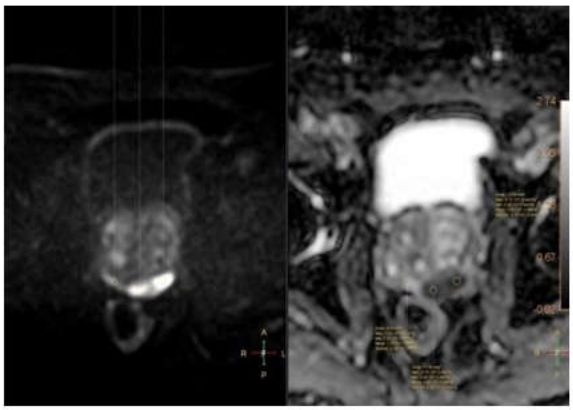

d

Figure 7 MpMRI examination of a 72-year-old patient with PSA 34 ng/ml; lesion was present in the left peripheral zone and the score was determined to be PI-RADS 5. Lesion exhibits extraprostatic extension. This is because the width of the surface that contacts the capsule is longer than 1 cm in the T2W image. After the TRUS-guided biopsy, Gleason score was reported as 3+4 for prostatic adenocarcinoma. **a)** Lobular-contour lesion (arrow) with regular margins at an approximate size of 22x11 mm was observed in the left posterior peripheral zone at prostate base level (T2W score P5). **b)** DWI with b1500; lesion is restricted**c)** Mean ADC value was measured as 0.50 in the ADC map (DWI score P5). **d)** DCE-MRI examination; Focal lesion with rapid and early contrast uptake as compared to the neighboring peripheral zone (Contrast uptake "+").

Comparing the specificity, sensitivity, positive predictive and negative predictive values of T2W, DWI, DCE-MRI and the MpMRI variables constituted by the combination of the former, the highest sensitivity and negative predictive value were seen in MpMRI. Although the highest specificity and positive predictive values were observed in DWI, the role of DWI in local staging is limited. In addition, a high negative predictive value is important for clinicians since MpMRI is frequently used to eliminate CSC. For these reasons, MpMRI is themost valuable method in diagnosis, staging, active follow-up and post-treatment follow-up of PCa.

The sensitivity of MpMRI in detecting low-volume Gleason 3+3 tumors is very low (35). In our study, there was only one patient with a biopsy result of Gleason 3+3, and the patient's PI-RADS assessment category was determined as PI-RADS category 2 and no suspicious lesions were detected. Although the inability to detect low-grade tumors in MpMRI is ironic, it seems like an advantage. These clinically insignificant tumors carry the concern of "overdiagnosis". Due to this property, it is possible to say that low-risk patients that do not exhibit any sings of tumor in MpMRI are suitable candidates for activefollow-up.

Our study had some limitations such as low number of patients, low number of transition zone lesions and the study being conducted in a single center. In addition, TRUS-guided 10 quadrant biopsy was blindly performed in a majority of the patients in our study, and the fact that biopsies will not exactly match the lesions in MpMRI as much as targeted biopsy or prostatectomy material is among the limitations.

CONCLUSION

It is seen that MpMRI is quite promising in detecting, localizing and characterizing the lesion, assessing the risk level in patients with suspected prostate cancer and in determining observation and patient selection strategies for biopsy in accordance with the risk level.

Due to the high sensitivity and negative predictive value of MpMRI in the diagnosis of prostate cancer, all patients with suspected PCa and especially those who did not have CSC in the first biopsy but are planned to have another biopsy due to suspected PCa can be recommended for evaluation with MpMRI before prostate biopsy. We think that MpMRI will increase patient compliance especially by decreasing the number of unnecessary biopsies as well as providing information that will reduce possible complications.

References

1. Siegel RL, Miller KD, Jemal A. Cancer statistics, 2016. *CA Cancer J Clin*. 2016;66:7- 30.
2. Siegel R, Naishadham D, Jemal A. Cancer statistics, 2013. CA: a cancer *journal for clinicians*.2013;63:11-30.
3. Ketelsen D, Röthke M, Aschoff P, Merseburger A, Lichy M, Reimold M, *et al*. Detection of bone metastasis of prostate cancer-comparison of whole-body MRI and bone scintigraphy. RoFo: Fortschritte auf demGebiete der Rontgenstrahlen und der Nuklearmedizin. 2008;180:746-52.
4. A.HeidenreichMB, S.Joniau, M.D.Mason, V.Matveev, N.Mottet, H-P.Schmid, T.H. van der Kwast, T. Wiegel, F. Zattoni. Guidelines on Prostate Cancer. *European Association of Urology*. January 2011;152:61-71.
5. Levine MA, Ittman M, Melamed J, Lepor H. Two consecutive sets of transrectal ultrasound guided sextant biopsies of the prostate for the detection of prostate cancer. *The Journal of urology*.1998;159:471-6.
6. Turkbey B, Pinto PA, Choyke PL. Imaging techniques for prostate cancer: implications for focal therapy. *Nature Reviews Urology*. 2009;6:191-203.
7. Weinreb JC, Barentsz JO, Choyke PL, Cornud F, Haider MA, Macura KJ, *et al*. PI- RADS prostate imaging–reporting and data system: 2015, version 2. *European urology*. 2016;69:16-40.
8. Hoeks CM, Barentsz JO, Hambrock T, Yakar D, Somford DM, Heijmink SW, *et al*. Prostate cancer: multiparametric MR imaging for detection, localization, and staging. *Radiology*.2011;261:46-66.
9. Hassanzadeh E, Glazer DI, Dunne RM, Fennessy FM, Harisinghani MG, Tempany CM. Prostate imaging reporting and data system version 2 (PI-RADS v2): a pictorial review. *Abdominal Radiology*.2017;42:278-89.
10. 113Siegel RL, Miller KD, Jemal A. Cancer Statistics. CA: a cancer journal for clinicians.2016;66:7-30.
11. Sahin H, Cetinkaya M, Deliktas H. ProstatKanserinde; Üriner, Serum veDoku Biyomarkerlerinde Yeni

Gelişmeler Nelerdir? UroonkolojiBulteni.2017; 16:95-100.
12. Roehrborn CG, Pickens GJ, Sanders JS. Diagnostic yield of repeated transrectal ultrasound-guided biopsies stratified by specific histopathologic diagnoses and prostate- specific antigen levels. *Urology*.1996; 47:347-52.
13. Stroumbakis N, Cookson MS, Reuter VE, Fair WR. Clinical significance of repeat sextant biopsies in prostate cancer patients. *Urology*.1997; 49:113-8.
14. Djavan B, Ravery V, Zlotta A, Dobronski P, Dobrovits M, Fakhari M, *et al*. Prospective evaluation of prostate cancer detected on biopsies 1, 2, 3 and 4: when should we stop? *The Journal of urology*. 2001; 166:1679-83.
15. Djavan B, Waldert M, Zlotta A, Dobronski P, Seitz C, Remzi M, *et al*. Safety and morbidity of first and repeat transrectal ultrasound guided prostate needle biopsies: results of a prospective European prostate cancer detection study. *The Journal of urology*. 2001; 166:2242-6.
16. Wilt TJ, Brawer MK, Jones KM, Barry MJ, Aronson WJ, Fox S, *et al*. Radical prostatectomy versus observation for localized prostate cancer. *New England Journal of Medicine*. 2012; 367:203-13.
17. Panebianco V, Barchetti F, Sciarra A, Ciardi A, Indino EL, Papalia R, *et al*., editors. Multiparametric magnetic resonance imaging vs. standard care in men being evaluated for prostate cancer: a randomized study. Urologic Oncology: Seminars and Original Investigations;2015;33:1-7.
18. Hricak H, Choyke PL, Eberhardt SC, Leibel SA, Scardino PT. Imaging prostate cancer: a multidisciplinary perspective. *Radiology*. 2007; 243:28-53.
19. Wu L-M, Xu J-R, Ye Y-Q, Lu Q, Hu J-N. The clinical value of diffusion-weighted imaging in combination with T2-weighted imaging in diagnosing prostate carcinoma: a systematic review and meta-analysis. *American Journal of Roentgenology*.2012; 199:103-10.
20. Yoshimitsu K, Kiyoshima K, Irie H, Tajima T, Asayama Y, Hirakawa M, *et al*. Usefulness of apparent diffusion coefficient map in diagnosing prostate carcinoma: correlation with stepwise histopathology. *Journal of Magnetic Resonance Imaging*. 2008; 27:132-9.
21. deSouza NM, Riches SF, Vanas NJ, Morgan VA, Ashley SA, Fisher C, *et al*. Diffusion-weighted magnetic resonance imaging: a potential non-invasive marker of tumour aggressiveness in localized prostate cancer. *ClinRadiol*.2008; 63:774-82.
22. Zelhof B, Pickles M, Liney G, Gibbs P, Rodrigues G, Kraus S, *et al*. Correlation of diffusion-weighted magnetic resonance data with cellularity in prostate cancer. *BJU international*.2009; 103:883-8.
23. Wu L-M, Xu J-R, Ye Y-Q, Lu Q, Hu J-N. The clinical value of diffusion-weighted imaging in combination with T2-weighted imaging in diagnosing prostate carcinoma: a systematic review and meta-analysis. *American Journal of Roentgenology*.2012; 199:103-10.
24. Vargas HA, Akin O, Franiel T, Mazaheri Y, Zheng J, Moskowitz C, *et al*. Diffusion- weighted endorectal MR imaging at 3 T for prostate cancer: tumor detection and assessment of aggressiveness. *Radiology*.2011; 259:775-84.
25. Kim CK, Park BK, Han JJ, Kang TW, Lee HM. Diffusion-weighted imaging of the prostate at 3 T for differentiation of malignant and benign tissue in transition and peripheral zones: preliminary results. *Journal of computer assisted tomography*.2007; 31:449-54.
26. Gibbs P, Pickles MD, Turnbull LW. Diffusion imaging of the prostate at 3.0 tesla. Investigative radiology. 2006;41:185-8.
27. Verma S, Turkbey B, Muradyan N, Rajesh A, Cornud F, Haider MA, *et al*. Overview of dynamic contrast-enhanced MRI in prostate cancer diagnosis and management. *American Journal of Roentgenology*.2012;198:1277-88.
28. Ocak I, Bernardo M, Metzger G, Barrett T, Pinto P, Albert PS, *et al*. Dynamic contrast-enhanced MRI of prostate cancer at 3 T: a study of pharmacokinetic parameters. *American Journal of Roentgenology*. 2007; 189:W192-W201.
29. Futterer JJ, Heijmink SW, Scheenen TW, Veltman J, Huisman HJ, Vos P, *et al*. Prostate cancer localization with dynamic contrast-enhanced MR imaging and proton MR spectroscopic imaging. *Radiology*. 2006; 241:449-58.
30. Tanimoto A, Nakashima J, Kohno H, Shinmoto H, Kuribayashi S. Prostate cancer screening: The clinical value of diffusion-weighted imaging and dynamic MR imaging in combination with T2-weighted imaging. *Journal of Magnetic Resonance Imaging*. 2007;25:146-52.
31. Futterer JJ, Briganti A, De Visschere P, Emberton M, Giannarini G, Kirkham A, *et al*. Can Clinically Significant Prostate Cancer Be Detected with Multiparametric Magnetic Resonance Imaging? A Systematic Review of the Literature. *European urology*. 2015; 68:1045-53.
32. Abd-Alazeez M, Kirkham A, Ahmed HU, Arya M, Anastasiadis E, Charman SC, *et al*. Performance of multiparametric MRI in men at risk of prostate cancer before the first biopsy: a paired validating cohort study using template prostate mapping biopsies as the reference standard. *Prostate cancer and prostatic diseases*.2014;17:40-6.
33. Stephenson AJ, Scardino PT, Eastham JA, BiancoJr FJ, Dotan ZA, DiBlasio CJ, *et al*. Postoperative nomogram predicting the 10-year probability of prostate cancer recurrence after radical prostatectomy. Journal of clinical oncology: official *journal of the American Society of Clinical Oncology*. 2005; 23:7005.
34. B.H. Park, H.G. Jeon, B.C. Jeong, S.I. Seo, H.M. Lee, H.Y. Choi, *et al.* Influence of magnetic resonance imaging in the decision to preserve or resect neurovascular bundles at robotic assisted laparoscopic radical prostatectomy**.** *J Urol*, 192 (2014), pp.82-88.
35. Barrett T. What is multiparametric-MRI of the prostate and why do we need it? ISSN: 1755-5191.2015; p1-7.

****